

where the "transport" relaxation time τ_{tr} is given by

$$\frac{1}{\tau_{tr}} = \frac{2\pi N}{\hbar} \sum_{k'} \delta(\epsilon_k - \epsilon_{k'}) |V_{k',k}|^2 (1 - \cos\theta_{k',k}). \quad (9)$$

One can put (8) in vector form:

$$\vec{\omega}_k = \Delta\vec{r}_k / \tau_{tr}, \quad \Delta\vec{r}_k \equiv \frac{1}{4}(\hbar/mc)^2 \vec{k} \times \vec{\sigma}. \quad (10)$$

Noting that $1/\tau_{tr}$ is a transport collision rate, one can interpret $\Delta\vec{r}_k$ as a side jump of the electron (occurring during each collision) in the direction perpendicular to both the spin and momentum vectors. The side jump $\Delta\vec{r}_k$ of (10) agrees with that given by Berger^{6a} assuming Born and short-range approximations, except that our result is larger by a factor of $\frac{3}{2}$.⁸ It is to be noted that the final form of the side jump $\Delta\vec{r}_k$ does not depend on either the magnitude or the form of the impurity potential. This is in agreement with Berger's result which is independent of the depth and radius of the scattering potential well.

The magnitude of the side jump can be estimated by assuming $k \approx 10^8 \text{ cm}^{-1}$ at the Fermi level:

$$|\Delta\vec{r}_k| \approx 4 \times 10^{-14} \text{ cm} \quad (11)$$

which is too small to explain the data.^{6a} However, as pointed out by Smit¹ and discussed by Berger,^{6a} the small effect of the spin-orbit interaction ($H_v^{s \cdot o}$) associated with the impurity potential should be replaced by the spin-orbit interaction ($H_U^{s \cdot o}$) associated with the periodic lattice

potential. The effect of $H_U^{s \cdot o}$ is to (electrically) polarize the electrons.⁹ The combined effect of the dipole moment and impurity potential is to produce an effective spin-orbit interaction,¹⁰ which is enhanced by a factor of 10^4 compared to $H_v^{s \cdot o}$; thereby enhancing the magnitude of the side jump by the same factor. A more detailed treatment of this enhancement effect will be postponed for forthcoming work.¹¹

*Work supported in part by the National Science Foundation under Grant No. 21 290, and the Office of Naval Research under Contract No. N00014-69-0200-4032.

¹J. Smit, *Physica (Utrecht)* **24**, 39 (1958).

²J. M. Luttinger, *Phys. Rev.* **112**, 739 (1958).

³J. Kondo, *Progr. Theor. Phys.* **27**, 772 (1962); F. E. Maranzana, *Phys. Rev.* **160**, 421 (1967).

⁴E. N. Adams and E. I. Blount, *J. Phys. Chem. Solids* **10**, 286 (1959).

⁵W. Kohn and J. M. Luttinger, *Phys. Rev.* **108**, 590 (1957).

^{6a}L. Berger, *Phys. Rev. B* **2**, 4559 (1970).

^{6b}L. Berger, *Phys. Rev. B* **5**, 1862 (1972).

⁷Cf. Ref. 2; a completely different derivation is given by S. K. Lyo, thesis, University of California, Los Angeles, 1972 (unpublished).

⁸This discrepancy is currently under investigation.

⁹R. C. Fivaz, *Phys. Rev.* **183**, 586 (1969).

¹⁰One has to assume a slowly varying condition for the impurity potential $V(\vec{r})$.

¹¹Ref. 7; S. K. Lyo and T. Holstein, to be published.

Coherent Scattering in a Random-Network Model for Amorphous Solids

P. Chaudhari, J. F. Graczyk, and H. P. Charbneau

IBM Thomas J. Watson Research Center, Yorktown Heights, New York 10598

(Received 30 June 1972)

Coherent scattering regions of approximately 10–25 Å in size have been observed in a variety of amorphous solids. It has been suggested that these observations provide evidence for the microcrystalline model. In this note we show that the observations of coherently scattering regions are not incompatible with a random-network model.

High-resolution dark-field electron microscopy of amorphous Si, Ge, Ge-Te alloys, and SiO₂ has revealed the presence of coherently scattering regions of approximately 10–25 Å in diameter.¹⁻⁵ In the case of amorphous silicon and germanium the coherently scattering regions (CSR's) cannot be related to the diamond cubic crystallites as the calculated interference functions do not agree with the experimental values.⁶⁻⁸ It has been sug-

gested, however, that the CSR correspond to the wurtzite-structure crystallites, and a better match with the calculated and experimental values of the interference function can then be obtained.⁵ An alternative approach which generates radial distribution functions that match the experimentally determined ones is to consider some form of a random-network model.⁹⁻¹⁵ In this, no structural order of the type present in the micro-

crystalline model¹⁶ is preserved and the atoms are arranged in a network. Scattering from such a model is usually expected to be homogeneous and this would appear to be in contradiction with the observations of CSR's. In this note we report on the results of our calculations on the scattering properties of a cluster of atoms whose coordinates are described on the basis of a random network.

The model for amorphous solids that we shall therefore be investigating here consists of the following. There are clusters of atoms which correspond to the size of the coherently scattering regions. The atomic arrangement in any given cluster is described by a random network. The clusters are distinguishable entities only in terms of coherent scattering. They are not separated by grain boundaries as in the microcrystalline model. In fact, the concept of a grain boundary is not physically meaningful other than in scattering since the boundary separates two clusters with atomic positions described by a random network. In scattering, the boundary has meaning since it separates two clusters which scatter coherently into two different regions of reciprocal space. If this model is a valid description, it is required to show that a cluster of atoms fulfilling the random network criterion also exhibits coherent scattering.

In order to do this we shall calculate the structure factor of a cluster of atoms which has been shown to yield a satisfactory radial distribution function. While the latter quantity yields an ap-

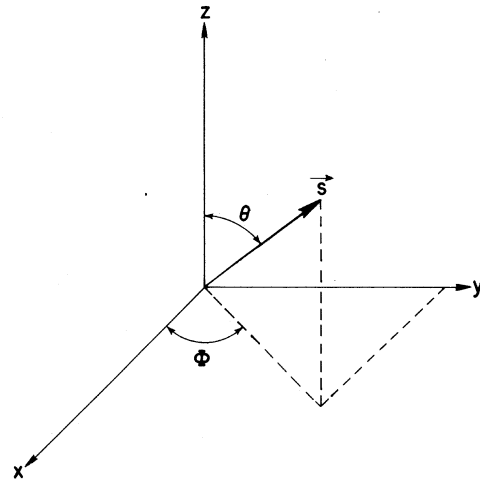


FIG. 1. Coordinate system utilized in computing FF^* . The scattering vector $\vec{s} = \vec{S} - \vec{S}_0$, θ , and Φ are shown in relation to an arbitrary orthogonal system x , y , and z .

propriate statistical average, the structure factor is more sensitive to deviations from average scattering. It is this deviation or structure which gives rise to the observation of CSR's. The structure factor is given by

$$F_t(\theta, \Phi, s) = \sum_m f_m \exp[(2\pi i/\lambda)(\vec{S} - \vec{S}_0) \cdot \vec{r}_m], \quad (1)$$

where the sum is over an aggregate of m atoms, $|\vec{s}| = 4\pi \sin(\theta)/\lambda = |\vec{S} - \vec{S}_0|$, and the coordinates (x, y, z) and the angles θ and Φ are shown in Fig. 1. The intensity is proportional to $F_t F_t^*$ and can be written as

$$F_t F_t^*(\theta, \Phi, s) = \sum_m \sum_n f_m f_n \exp[(2\pi i/\lambda)(\vec{S} - \vec{S}_0) \cdot \vec{r}_{mn}], \quad (2)$$

where $\vec{r}_{mn} = \vec{r}_m - \vec{r}_n$. For our purpose it is convenient to express Eq. (2) in the following form:

$$F_t F_t^*(\theta, \Phi, s) = K f f^* FF^*(\theta, \Phi, s),$$

where

$$FF^*(\theta, \Phi, s) = \sum_m \sum_n \exp(2\pi i/\lambda) |\vec{S} - \vec{S}_0| [(x_m - x_n) \sin\theta \cos\Phi + (y_m - y_n) \sin\theta \sin\Phi + (z_m - z_n) \cos\theta]. \quad (3)$$

As ff^* is a rapidly decreasing and well-behaved function of s , the calculated function FF^* will be of larger amplitude for large values of s but it will contain the same structural information as $F_t F_t^*$.

The calculations that we report on here were carried out on a model for amorphous silicon and germanium generated by Henderson and Herman.¹⁴ These authors have shown that a cluster of 64 atoms—approximately equal to the number of atoms in a CSR—generates a radial distribu-

tion function which matches that of amorphous silicon and germanium. We have used their coordinates of the 64 atoms to calculate FF^* .

The calculations were performed first for a fixed value of the length of the scattering vector $|\vec{s}| = 4\pi \sin(\theta)/\lambda (\text{\AA}^{-1})$. This magnitude was equal to the experimentally determined value corresponding to the first intense halo in the diffraction pattern of amorphous germanium. This value is close to the scattering vector correspond-

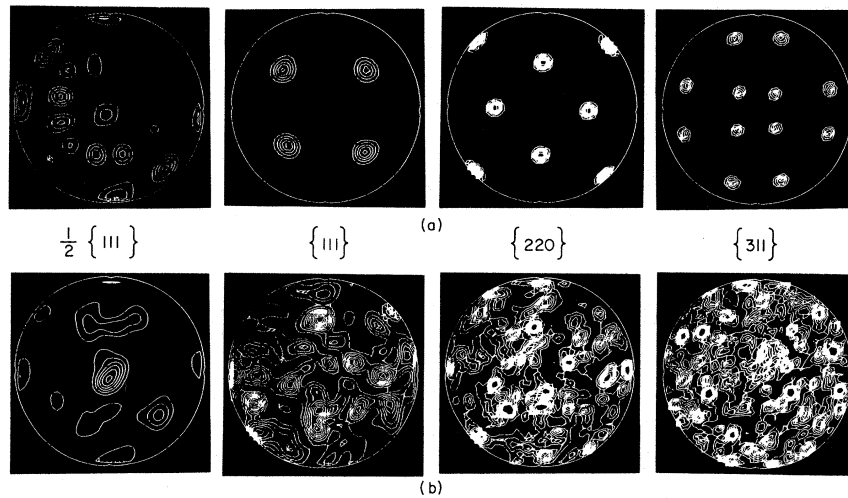


FIG. 2. Equivalent contour maps of the calculated values of FF^* for a fixed value of $|\vec{s}|$ equal to $\frac{1}{2}\{111\}$, $\{111\}$, $\{220\}$, and $\{311\}$ plotted as a function of θ and Φ . θ varies radially outward from 0° to 90° and Φ varies circumferentially from 0° to 360° . The contours are values of FF^* in equal increments of 0.1; for (a), the crystalline case, the gain is 1; for (b), the random-network case, the gain is 10.0, except for the $\frac{1}{2}\{111\}$ for which the gain is 1.0.

ing to the crystalline $\{111\}$ reflection. Other fixed values of the scattering vector for which similar calculations were repeated are $\frac{1}{2}\{111\}$, $\{220\}$, and $\{311\}$. Using these values of the magnitude of the scattering vector, the structure factor was calculated as a function of θ and Φ over the range $\theta = 0^\circ$ to 90° and $\Phi = 0^\circ$ to 360° . In order to compare these results with a diamond crystallite the structure factor was calculated also for a crystal containing 64 atoms. These results are shown in Figs. 2(a) and 2(b).

It is readily apparent that the random-network model investigated here does not contain the symmetry properties of the crystallite. However, there are distinct local maxima in intensity. Presumably, if these maxima are sufficiently large compared to the background the imaging technique used in dark-field electron microscopy will show them as CSR's. In this calculation the ratio of maximum value of FF^* for amorphous and diamond-crystalline germanium was found to be 0.16, 0.15, and 0.28 for $\{111\}$, $\{220\}$, and $\{311\}$. Experimentally, the observations on CSR's performed in this laboratory do indeed show them to be less intense than their crystalline form. There is, however, no quantitative determination of the intensity ratio.

The variation in the structure factor with the magnitude of the scattering vector for amorphous and crystalline models with 64 atoms is shown in Figs. 3(a) and 3(b). The values of θ and Φ were selected to give a maximum intensity at the $\{111\}$

position. We note that the intensity for both the amorphous and crystalline models varies between zero and a well-defined maximum. It suggests that the background intensity in relation to the maximum is sufficiently small that the coherently scattering regions associated with either of the two models should be detectable. We conclude, therefore, that in the amorphous model investigated here the presence of the coherently scattering regions is not incompatible with a random-network model.

The following model for amorphous materials such as Si, SiO_2 , Ge, and Ge-Te alloys is therefore suggested. The solids are composed of clusters of atoms. The clusters are recognized as entities from the nature of their localized scattering into reciprocal space. However, the coordinates of atoms in a given cluster are not known. Both the microcrystalline models^{5,16,17} and a random-network model¹⁴ are capable of generating coherent scattering regions.

Our objection to the perfect microcrystallite model surrounded by a grain boundary is that it ignores the distortions introduced at the grain boundary when two microcrystallites join together. If we assume that the width of the grain boundary is 3 Å and the microcrystallite is 15 Å, the distortions are likely to go through the crystallite. If we accept the presence of these distortions, the coordinates of the atoms are no longer defined by a crystallite model. At best, the crystallite model can serve as a reference

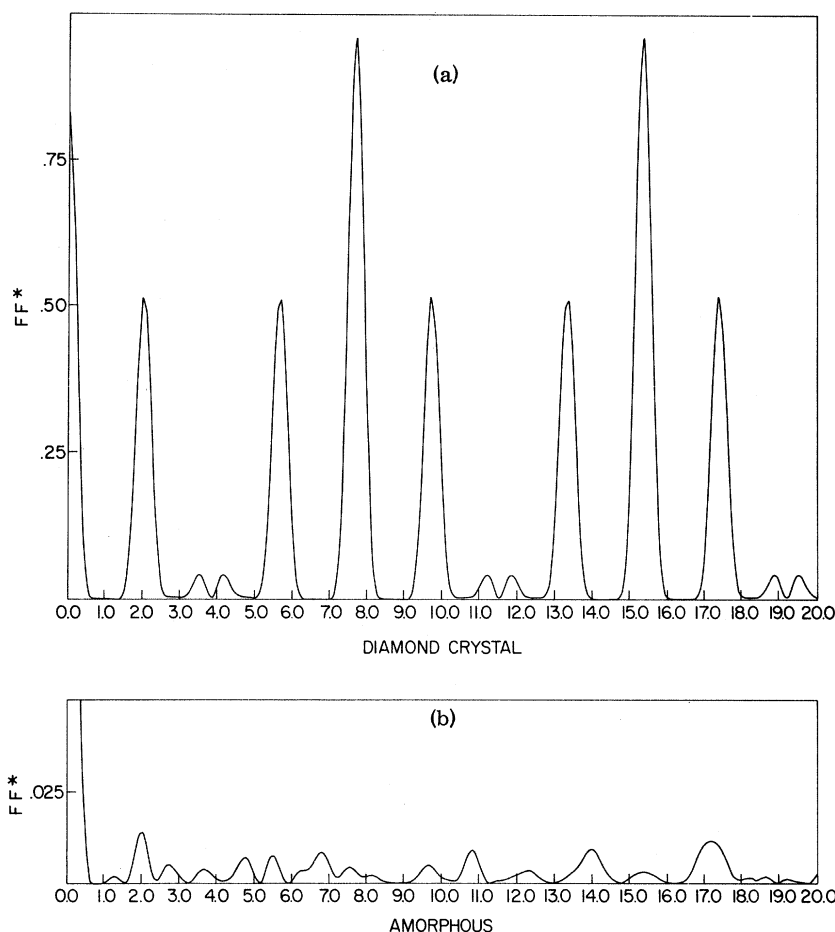


FIG. 3. Variation in FF^* as a function of the scattering vector $|\vec{S}|$ for fixed θ and Φ . (a) Crystalline model; (b) random-network model.

point and we are back to the problem of determining the coordinates of atoms without knowing the nature of the distortions. It is probable that the reason why a random-network model can lead to coherent scattering lies in the technique with which the coordinates of atoms are generated. Using a periodic boundary condition, Henderson and Herman¹⁴ allowed the atoms in germanium and silicon to relax from their crystalline positions towards a random structure. The reference or starting point is still the diamond structure. This approach may therefore be a suitable way of generating the structure of amorphous silicon, germanium, and other materials. It is, of course, important to recognize that the observations of coherent scattering regions rule out the possibility of a continuous random network which generates uniform scattering.

The authors would like to thank Dr. D. Henderson of IBM San Jose for kindly supplying the coordinates for the 64 atomic positions in the ran-

dom-network model. The authors also acknowledge many stimulating discussions with Professor D. B. Dove of the University of Florida during the incubation stage of this work.

¹M. Tanaka, *Jap. J. Appl. Phys.* **10**, 274 (1971).

²M. L. Rudee, *Phys. Status Solidi (b)* **46**, K1 (1971).

³P. Chaudhari and S. R. Herd, *J. Non-Cryst. Solids* **8/9**, 56 (1972).

⁴P. Chaudhari, J. F. Graczyk, and S. R. Herd, *Phys. Status Solidi (b)* **51**, 1068 (1972).

⁵M. L. Rudee and A. Howie, *Phil. Mag.* **25**, 1001 (1972).

⁶S. C. Moss and J. F. Graczyk, in *Proceedings of the Tenth International Conference on the Physics of Semiconductors, Cambridge, Massachusetts, 1970*, edited by S. P. Keller, J. C. Hensel, and F. Stern, CONF-700801 (U.S. AEC Division of Technical Information, Springfield, Va., 1970), p. 658.

⁷J. Chang and D. B. Dove, in *Proceedings of the Sev-*

enth International Conference on Electron Microscopy, Grenoble (Société Française de Microscopie Electronique, Paris, 1970), Vol. , p. 133.

¹⁰B. E. Warren, Z. Krist. **86**, 349 (1933).

¹¹D. E. Polk, J. Non-Cryst. Solids **5**, 365 (1971).

¹²F. Betts and A. I. Bienenstock, Bull. Amer. Phys. Soc. **17**, 31 (1972).

¹³N. J. Shevchik, Bull. Amer. Phys. Soc. **16**, 347 (1971).

¹⁴D. Henderson and F. Herman, to be published.

¹⁵R. Grigorovici and R. Manaila, J. Non-Cryst. Solids **1**, 371 (1969).

¹⁶A. A. Lebedev, N. N. Valenkov, and E. A. Porai-Koshito, quoted by K. S. Evstropiyet, in *Proceedings of the Conference on the Structure of Glass, Leningrad, 1953* (Consultants Bureau, New York, 1958), p. 9.

¹⁷J. H. Koenert and J. Karle, Nature (London), Phys. Sci. **236**, 92 (1972).

Magnetic Hyperfine Modulation of Dye-Sensitized Delayed Fluorescence in an Organic Crystal

R. P. Groff, R. E. Merrifield, A. Suna, and P. Avakian

Central Research Department, E. I. du Pont de Nemours and Company, Wilmington, Delaware 19898

(Received 1 June 1972)

Magnetic fields were found to decrease rhodamine-*B*-sensitized delayed fluorescence in anthracene by up to 60% at 10 mTorr. An inverse but smaller effect was found on sensitized photoconductivity. The observations are explained in terms of a magnetic-field-dependent recombination of surface electrons and injected holes, with the field scale being fixed by hyperfine interactions.

We report a new effect of magnetic fields on delayed fluorescence in organic crystals at room temperature. Magnetic modulation of the intensity of delayed fluorescence from an anthracene crystal by as much as 75% results when triplet excitons are injected into the crystal from an adsorbed layer of the sensitizing dye, rhodamine *B*. In its response to a magnetic field, dye-sensitized delayed fluorescence differs from that produced by direct optical excitation of the crystal in that appreciable modulation is produced by much smaller fields, e.g., a field of 10 mTorr (100 Oe) changes the output intensity by 60% compared with a 2% change for an unsensitized crystal. In view of the field strength over which this modulation occurs, we call it hyperfine modulation (HFM). A similar field dependence (but smaller in amplitude and of opposite sense) has also been observed on rhodamine-*B*-sensitized photoconductivity. We believe these phenomena result from field-dependent surface recombination of electrons and holes.

Anthracene crystals were sensitized with rhodamine *B* following the procedure of Nickel, Staerk, and Weller,¹ and the sample was placed between the pole pieces of an electromagnet.

The solid line of Fig. 1 shows the magnetic field dependence of rhodamine-*B*-sensitized delayed fluorescence (excited at 570 nm) in anthracene. The magnetic field was applied parallel to the *a* axis with the exciting light incident normal

to the *ab* plane. As the field is increased, the sensitized emission increases at first, reaching a maximum ca. 1% above its zero-field value at 0.3–0.7 mTorr. Further field increases result in a monotonic decay toward saturation at 20–30 mTorr. The overall amplitude of the effect depends on sample history and preparation. The dashed line of Fig. 1 shows the field dependence of delayed fluorescence from direct excitation of triplet excitons (680 nm light) in the same crystal.^{2,3} This field dependence has been adequately

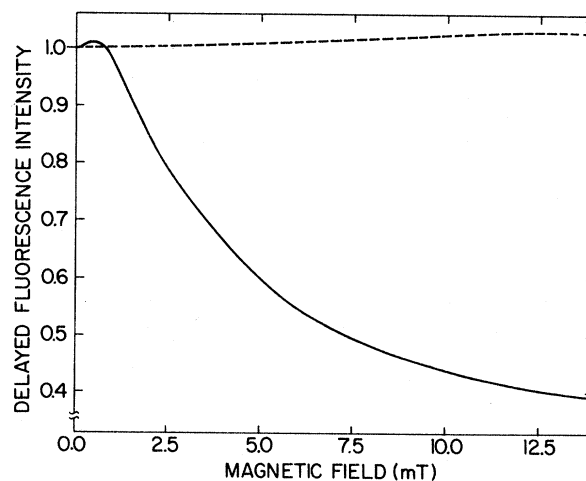


FIG. 1. Observed magnetic field modulation of normalized delayed fluorescence intensity; solid line, 570-nm excitation; dashed line, 680-nm excitation.